JOURNAL OF GEOPHYSICAL RESEARCH, VOL. 93, NO. B12, PAGES 15,153–15,162, DECEMBER 10, 1988

Terrestrial Heat Flow Above the Andean Subduction Zone in Bolivia and Peru

STEVEN G. HENRY[1] AND HENRY N. POLLACK

Department of Geological Sciences, University of Michigan, Ann Arbor

We report 35 new and 9 revised terrestrial heat flow measurements overlying the Andean subduction zone in Bolivia and Peru. The measurement sites are distributed in the Andean Cordillera, the Altiplano, the sub-Andean ranges, and the sedimentary platform and basins to the east of the Andes. They fall in the distance range 75–900 km from the Peru-Chile trench. Sites in the Peruvian Cordillera have a mean heat flow of 41 mW m^{-2}, whereas those in the Bolivian Cordillera and Altiplano average 84 mW m^{-2}. The sub-Andean ranges and the adjacent sedimentary platform have a mean heat flow of 50 mW m^{-2}. The higher heat flow of the Bolivian Cordillera and Altiplano lies to the east of Quaternary volcanoes along the Bolivia-Chile border and in southernmost Peru and thus can be recognized as a "back arc" heat flow high. Neither Quaternary volcanism nor high heat flow are present in central and northern Peru. This contrasting along-strike pattern correlates with the variable angle of subduction of the Nazca plate beneath the region. Beneath Bolivia the subduction is at about 30°–35°, whereas beneath Peru it is subhorizontal and may be providing a cold underplate to the overlying Peruvian lithosphere. Extensive Miocene volcanism in Peru suggests, however, that heat flow in Peru 10 Ma ago was likely similar to that in Bolivia in the present day and implies a change in subduction and a rapid diminution of heat flow in Peru over the past 10 Ma. Imbrication of cold oceanic lithosphere beneath Peru, analogous to that beneath western British Columbia, may provide a mechanism for rapid reduction of the heat flow.

INTRODUCTION

We report 35 new heat flow measurements overlying the Andean subduction zone in Bolivia and Peru. The measurements include 20 of the conventional type and 15 in petroleum fields using bottom hole temperatures, stratigraphic data, and well cuttings. We also have applied topographic corrections to measurements at nine Andean sites published earlier by other investigators to yield revised values. The locations of the measurements are shown in Table 1 and Figure 1, and details of the measurements are provided in Table 2.

The Andean subduction zone is perhaps the best present-day example of the interaction of oceanic and continental lithosphere in a zone of convergence and differs significantly from the subduction zones of the western Pacific where the convergent interaction is characteristically between oceanic plates and associated island arcs. Prior to 1978 the only heat flow determinations in western South America were in Lake Titicaca [*Sclater et al.*, 1970] and in northwestern Colombia, [*Sass et al.*, 1974]. An extensive reconnaissance investigation by S. Uyeda and colleagues resulted in estimates of heat flow at 20 sites in Chile, Argentina, Bolivia, Peru, and Ecuador [*Uyeda et al.*, 1978*a*, *b*, 1980; *Watanabe et al.*, 1980; *Uyeda and Watanabe*, 1982]. Some of the reconnaissance values reported by Uyeda and colleagues require corrections to the measured temperature distributions because of the effects of the local topography and the uplift and erosional history which created the topography. In the rugged terrain of the Andes, uncorrected values are in some circumstances only very rough estimates and should be treated cautiously in tectonic interpretations. Accordingly, we have, where possible, applied topographic corrections to the reconnaissance values reported by Uyeda and colleagues.

[1]Now at Conoco Incorporated, Houston, Texas.

Paper number 88JB03485.
0148-0227/88/88JB-03485$05.00

TEMPERATURE MEASUREMENTS

Field Measurements

Temperature measurements were obtained in the field from February through December 1979 and June through August 1981, using electrical resistance thermometers with sensitivity of 0.01 K. Temperatures were measured principally in boreholes which were drilled for mineral exploration by the mining industry, although some measurements were made in petroleum boreholes. Useful observations were obtained in a total of 80 boreholes that ranged from vertical, through all inclinations, to horizontal in underground mines. Temperatures were recorded at 10-m intervals in the vertical and steeply inclined boreholes and at 5-m intervals in the horizontal boreholes. Temperatures in the horizontal boreholes in mines were measured from the mine walls to a distance of between 50 and 100 m. In most mines, equilibrium temperatures appeared to be reached at distances of about 30 m from the walls; however, this varied from mine to mine depending upon the time that the gallery had been open. In all but one mine the temperature distribution obtained from the horizontal boreholes was verifiable to some extent through gradients determined from vertical or inclined boreholes. Catavi (site 19), a mine with horizontal boreholes only, had temperature measurements made on 12 levels of the mine which provided adequate vertical distribution.

The quality of the subsurface temperature measurements may be visualized from the temperature versus depth profiles shown in Figure 2. A typical profile from each of the heat flow sites, with vertical or inclined boreholes greater than approximately 100 m in length, is displayed below the depth of near-surface disturbances. The temperature measurements in boreholes within underground mines are plotted at their distances from the overlying surface. For vertical boreholes this display is equivalent to a conventional temperature versus depth profile but beginning at the collar depth of the borehole. For horizontal and gently inclined boreholes at shallow depths within a mine, a plot of temperature versus depth beneath the

TABLE 1. Heat Flow Sites in Peru and Bolivia

Site Number	Site Name	South Latitude	West Longitude	Elevation, m	Tectonic Setting	Heat Flow Method	Heat Flow, mW m^{-2}	Distance From Trench, km
1	Pena Negra	4°17′	81°10′	200	SB	1	37	85
2	Lobitos	4°27′	81°16′	200	SB	1	28	90
3	Lomitos	4°37′	81°17′	200	SB	1	35	75
4	La Granja	6°35′	79°07′	2300	C	2	39	275
5	Marcahui	15°31′	73°45′	2600	C	2	44	175
6	Tintaya	14°54′	71°21′	4100	C	2	32	400
7	Cerro Verde	16°33′	71°34′	2700	C	2	44	205
8	Toquepala	17°16′	70°39′	3100	C	1	66	270
9	Capahuari Group	2°33′	76°08′	230	SB	3	52	625
	Capahuari	2°48′	76°27′	250				
	Forestal	2°21′	76°10′	220				
	Hiviyacu S.	2°30′	76°09′	240				
	Baratra	2°29′	75°38′	200				
	Huayuri S.	2°38′	76°14′	250				
10	Pavayacu	3°24′	75°23′	235	SB	3	53	765
11	Corrientes	3°51′	75°03′	160	SB	3	50	795
12	Yanayacu	4°54′	74°56′	145	SB	3	55	775
13	Yurimaguas	5°49′	76°08′	277	SB	3	55	610
14	Matilde	15°46′	69°03′	4300	C	2	106	500
15	Cuatro Amigos	15°47′	69°01′	4400	C	2	99	485
16	Colquiri	17°23′	67°08′	4200	C	2	75	535
17	Huanuni	18°17′	66°50′	4400	C	2	112	505
18	Bolivar	18°28′	66°50′	4100	C	2	109	500
19	Catavi	18°25′	66°35′	4400	C	2	66	550
20	Nasama	19°23′	67°11′	3840	A	2	83	440
21	Agua de Castilla	21°02′	66°35′	3880	A	1	75	500
22	Chorolque	20°54′	66°04′	4800	C	2	70	540
23	Tatasi	21°10′	66°08′	4200	C	2	94	525
24	Chilcobija	21°15′	66°03′	3940	C	2	70	550
25	Kolpani	21°18′	66°41′	3910	A	1	94	475
26	Yapacani	17°06′	64°04′	237	SA	3	59	835
27	Caranda	17°32′	63°32′	359	SA	3	50	850
28	Colpa	17°31′	63°16′	340	SA	3	56	885
29	La Pena Group	17°56′	63°01′	365	SA	3	53	900
	Paurito	17°41′	63°00′	362				
	Santa Cruz	17°48′	63°08′	400				
	La Pena	17°52′	62°57′	346				
	Palmar	17°59′	63°04′	371				
	Almendro	18°04′	63°02′	375				
	Rio Grande	18°14′	62°53′	340				
30	El Espino	19°18′	63°13′	715	SA	3	54	850
31	Camiri	20°01′	63°34′	870	SA	3	33	805
32	Mandeyapecua Group	20°26′	63°12′	840	SA	3	55	840
	Cambeiti	20°10′	63°11′	985				
	Boyuibe	20°25′	63°14′	823				
	Mitaigua	20°27′	63°08′	712				
	Mandeyapecua	20°27′	63°04′	732				
	Buena Vista	20°40′	63°21′	960				
33	Vuelta Grande	20°56′	63°11′	580	SA	3	50	850
34	Camatindi	20°59′	63°27′	1475	SA	3	47	805
35	Barredero	22°46′	64°17′	750	SA	3	27	710
A	San Fernando	3°08′	79°15′	3600	C	2	55	310
B	Raura	10°29′	76°45′	4800	C	2	17	300
C	Casapalca	11°39′	76°14′	4700	C	...	...	
D	Condestable	12°41′	76°36′	450	C	2	35	200
E	Cuajone	17°04′	70°46′	3500	C	2	57	255
F	Chojilla	16°25′	67°44′	2000	C	2	68	570
G	Corocoro	17°11′	68°30′	3900	A	...	...	
H	Chacarilla	17°34′	68°14′	3800	A	2	73	420
I	Santa Fe	18°10′	66°49′	4350	C	2	90	500

The tectonic setting codes are defined in Figure 1. The heat flow method codes are 1, *Bullard* [1939]; 2, *Henry and Pollack* [1985]; 3, modified BHT (this paper). Value of heat flow shown corresponds to value listed under q in Table 2 or under $q(u/e)$ in Table 2 if an uplift-erosion correction was applied. Dots indicate that heat flow could not be reliably determined.

topographic surface typically shows some curvature and usually indicates the need for topographic corrections.

The temperature distributions recorded during the field measurements provided observational constraints for the terrain correction modeling, which yields the vertical heat flow that would exist in the absence of any topographic perturbations or that would be found at a depth great enough to avoid significant horizontal components of the temperature

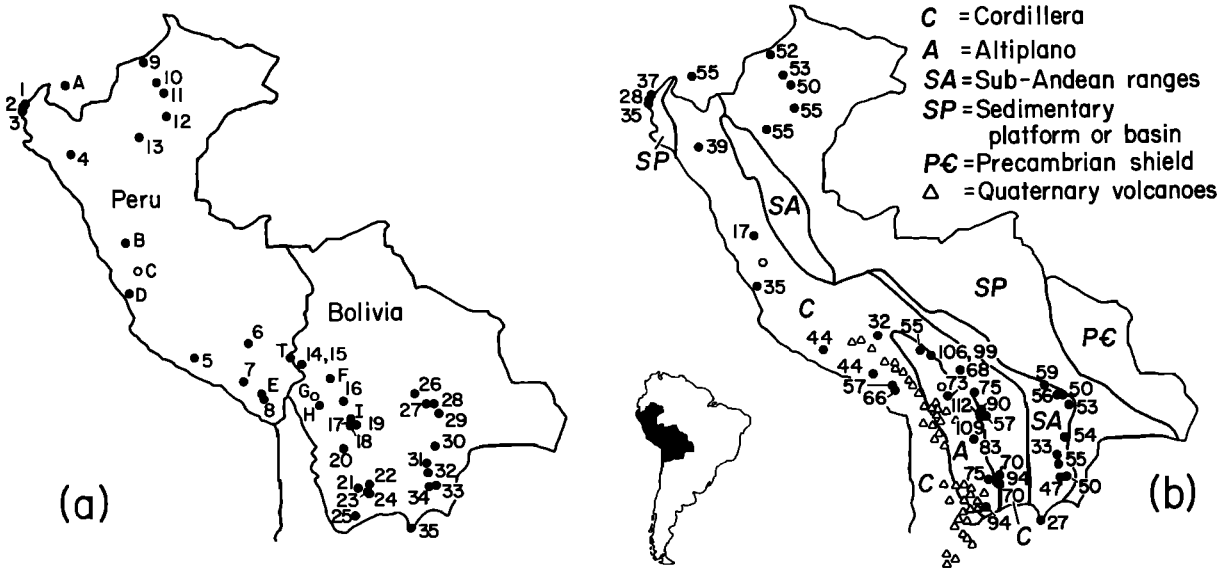

Fig. 1. (*a*) Map of Peru and Bolivia showing the locations of new heat flow sites (numbered solid circles), revised heat flow sites (lettered solid circles), and reevaluated heat flow sites where uncertainty of the heat flow estimates probably exceeds traditional bounds of reliability (open circles). Numbers and letters refer to site identification in Tables 1 and 2. (*b*) Heat flow values, in milliwatts per square meter, displayed against background of principal tectonic elements of the region. Heat flow at sites in the Cordillera and Altiplano was determined by conventional methods; heat flow at other sites was determined from bottom hole temperatures and well cuttings from petroleum boreholes.

gradient caused by topography. Some of the heat flow sites established in this investigation did not require topographic corrections, and the measured gradient is assumed to be the true gradient. Examples of these true gradients are shown in Figure 2 for sites 1, 2, 3, 8, 21, and 25.

Notably absent from the list of heat flow sites are the principal mines of the Central Mining District of Peru: Morococha, Yauricocha, Casapalca, and San Cristobal (Andayachagua). We visited each of these mines and made extensive measurements, but all yielded very poor results, including negative temperature gradients in places. The problems are almost surely related to water circulation, both natural and induced in the permeable Cretaceous limestones. Large drainge tunnels have been constructed under these mines for the purpose of lowering the water table to a level beneath the mining activity. The water flow in the tunnels is large and fluctuates seasonally, suggesting an easy infiltration and circulation of water through the country rock that severely perturbs subsurface temperatures, particularly along fracture zones and vertical conduits such as boreholes. We believe no reliable estimates of heat flow can be obtained in the Central Mining District of Peru. *Uyeda et al.* [1980] also attempted measurements at Yauricocha and Casapalca, and encountered similar difficulties. They do, however, report an unusually high temperature gradient and heat flow estimate for Casaplaca on the basis of a small subset of observations, but we believe that all temperatures in the Central Mining District are likely to be significantly perturbed and are therefore probably not reliable for heat flow determinations.

Bottom Hole Temperature Data

Bottom hole temperature (BHT) data were collected from the archives of the Peruvian national petroleum company, PETROPERU, and the Bolivian national petroleum company, Yacimientos Petroliferos Fiscales Bolivianos. The petroleum boreholes in Bolivia and Peru are principally to the east of the main Andean Cordillera (see Figure 1) and are generally deep (1–4 km) with respect to the relief of the surrounding terrain so that the temperatures at depth are not disturbed by the local topography. Sites 1, 2, and 3 located near the Peruvian coast are also petroleum boreholes, but the temperatures in these holes were logged by us; BHTs were not used. Deep exploration wells may have a few temperatures recorded at different depths, and so a rough temperature-depth profile may be obtained. The BHT data from several wells in the same field or from several nearby fields also provide a number of temperature measurements at different depths. The average geothermal gradient can be estimated from BHT observations from the slopes of the best fitting lines of the subsurface temperatures.

We examined more than a thousand BHTs from 176 fields in Bolivia and Peru, but quality control considerations enabled the determination of heat flow in only 15 fields. We applied the following criteria to determine whether a given field qualified for a heat flow determination: (1) eight or more BHTs were distributed over at least a 500-m depth range, (2) the slope of the least squares line fit to the BHT observations had a standard deviation of less than 10%, (3) the stratigraphy of the depth range for which the temperature gradient was calculated was well known, and (4) samples of the formations and lithologies encountered were available for measurement of thermal conductivity.

It is well known that during the drilling of petroleum wells, the circulation of the drilling fluid disturbs the equilibrium temperatures of the surrounding rock in such a way that the temperature gradient within the drilling fluid and in the rocks that are in contact with the fluid is lower than the equilibrium gradient. The magnitude of the drilling disturbance at a given depth is a function of the difference between the temperature of the rock and the temperature of the drilling fluids and of the length of time that the rocks have been disturbed. Various authors have modeled this disturbance (see the recent treat-

TABLE 2. Summary of Heat Flow Data

Site Number	Site Name	N	Maximum Depth, m	Temperature Gradient, K km^{-1}	n	Thermal Conductivity, W m^{-1} K^{-1}	q, mW m^{-2}	$q(u/e)$, mW m^{-2}	Estimated Uncertainty, ±%
				Conventional Sites (No Topographic Correction Required)					
1	Pena Negra	1	660	20.2	15	1.8 (2.3)	37 (46)		15
2	Lobitos	1	660	17.1	14	1.6 (2.0)	28 (34)		15
3	Lomitos	1	550	15.1	12	2.3 (2.9)	35 (44)		15
8	Toquepala	5	820	17.5	18	4.3	75	66	5
21	Agua de Castilla	1	110	37.5	6	2.0	75		10
25	Kolpani	2	150	52.4	18	1.8	94		10
				Conventional Sites (Topographic Correction Applied)					
4	La Granja	1	270	15.0	4	3.0	45	39	20
5	Marcahui	1	110	20.8	4	2.4	50	44	20
6	Tintaya	8	820	13.8	33	2.9	40	32	15
7	Cerro Verde	17	230	12.4	36	4.1	52 (41)	44	10
14	Matilde	2	130	33.3	4	3.6	120	106	25
15	Cuatro Amigos	2	230	34.2	16	3.3	113	99	10
16	Colquiri	3	320	21.0	15	4.2	88	75	5
17	Huanuni	6	900	17.1	5	8.3	142	112	5
18	Bolivar	6	400	26.1	29	4.9	128	109	10
19	Catavi	18	640	20.6–13.0	14	3.4–5.4	80 (159)	66	20
20	Nasama	1	70	36.1	7	2.3	83		10
22	Chorolque	4	760	18.3	7	4.9	88	70	10
23	Tatasi	5	350	39.6	38	2.7	107	94	10
24	Chilcobija	1	75	22.9	4	3.5	80	70	15
				Revised Conventional Sites (Topographic Correction Applied)					
A	San Fernando	1	75	26.3		2.4	63 (66)	55	15
B	Raura	4	146	6.4		3.9	25 (30)	17	20
C	Casapalca		654	74.0	1	2.6	··· (196)		···
D	Condestable	9	167	15.8	3	2.4	38 (24)	35	10
E	Cuajone	4	290	14.6	11	3.9	66 (98)	57	15
F	Chojilla	3	600	21.7		3.5	76 (68)	68	10
G	Corocoro	2	485	43.8	2	3.2	··· (183)		···
H	Chacarilla	5	150	27.0	7	2.7	73 (137)		20
I	Santa Fe		213	30.9		3.4	105 (126)	90	30
				Petroleum Field Sites					
9	Capahuari Group	92	4296	28.8 (24.0)	57	1.8 (2.2)	52 (53)		20
	Capahuari	34	4296						
	Forestal	15	3653						
	Hiviyacu S.	19	3322						
	Baratra	10	2767						
	Huayuri S.	14	3463						
10	Pavayacu	23	3436	29.7 (25.1)	18	1.8 (2.2)	53 (55)		20
11	Corrientes	32	3832	27.8 (23.3)	28	1.8 (2.2)	50 (51)		20
12	Yanayacu	10	3727	26.3 (22.3)	10	2.1 (2.7)	55 (60)		20
13	Yurimaguas	9	2312	32.4 (26.2)	17	1.7 (2.1)	55 (55)		20
26	Yapacani	8	3040	25.6 (21.2)	24	2.3 (2.9)	59 (62)		20
27	Caranda	141	2513	19.4 (15.3)	48	2.6 (3.2)	50 (49)		20
28	Colpa	77	3140	22.5 (18.9)	40	2.5 (3.1)	56 (59)		20
29	La Pena Group	144	3941	21.1 (17.5)	65	2.5 (3.2)	53 (56)		20
	Paurito	4	3315						
	Santa Cruz	13	3811						
	La Pena	42	3776						
	Palmar	15	3806						
	Almendro	3	3879						
	Rio Grande	67	3941						
30	El Espino	18	5214	20.7 (17.1)	48	2.6 (3.3)	54 (56)		20
31	Camiri	80	1845	13.7 (11.1)	17	2.4 (3.0)	33 (33)		20
32	Mandeyapecua Group	51	4000	21.1 (17.5)	70	2.6 (3.3)	55 (58)		20
	Cambeiti	15	1764						
	Boyuibe	10	4000						
	Mitaigua	6	2912						
	Mandeyapecua	8	3543						
	Buena Vista	12	1735						
33	Vuelta Grande	15	3233	18.4 (14.0)	32	2.7 (3.5)	50 (49)		20
34	Camatindi	20	1839	22.5 (19.9)	33	2.1 (2.6)	47 (52)		20
35	Barredero	12	1415	12.9 (10.4)	21	2.1 (2.6)	27 (27)		20

N is the number of boreholes at each site that yielded reliable temperature observations, either conventional or BHT; n is the number of thermal conductivity determinations for each site. Parenthetic values of temperature gradient, thermal conductivity, and heat flow at petroleum field sites and sites 1, 2, and 3 are values prior to corrections for the drilling disturbance and in situ porosity. Parenthetic values of heat flow at lettered sites and sites 7 and 19 are values (uncorrected for topography) reported by *Uyeda and Watanabe* [1982]. All heat flow values in the cordillera were corrected for the transient effects of uplift and erosion; these values are shown under column $q(u/e)$. Dots indicate that heat flow could not be reliably determined.

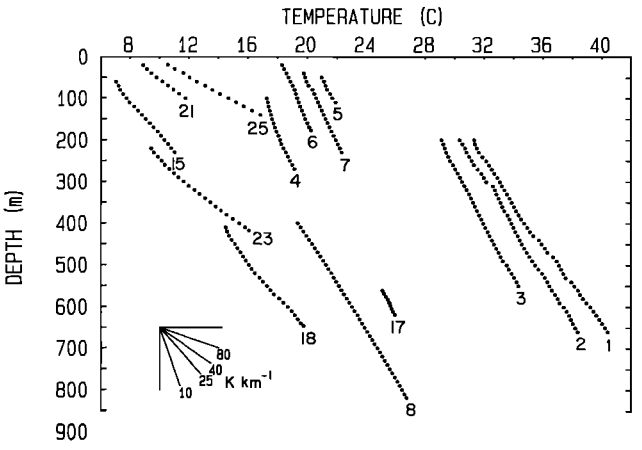

Fig. 2. Representative profiles of temperature versus depth beneath surface from 14 conventional heat flow sites in Bolivia and Peru. Numbers correspond to site numbers in Tables 1 and 2. Some profiles have been displayed to slightly higher or lower temperatures to avoid overlap with other profiles. Fan of slopes shows various temperature gradients in kelvins per kilometer.

ment of BHT stabilization by *Shen and Beck* [1986], in which there are references to all earlier major investigations of this subject). The usefulness of the corrections which result from the modeling of the equilibration process, however, is usually limited by a lack of sufficient temperature measurements in the disturbed period and/or knowledge about significant variables. Only in a situation where the fluid flow rates, temperatures and thermal properties of the fluid, and an accurate drilling history are well known will the correction determined from the modeling be able to estimate accurately the equilibrium temperatures and temperature gradient.

A statistical parametric method for estimating corrections to nonequilibrium BHT measurements has also been devised by the *American Association of Petroleum Geologists* [1976] (see *Speece et al.* [1985] for a discussion of this correction). The magnitude of this correction depends only on a single parameter, the depth of measurements. Because for nearly all of the BHTs we obtained in Bolivia and Peru no additional information except the depth of measurement was available, we applied the American Association of Petroleum Geologists (AAPG) correction (regionally adjusted) to the observed BHTs. While the probability of significant error is high if a gradient estimate is made on the basis of a single temperature observation corrected by this method, the application of the correction to an ensemble of BHTs in a given field will likely yield a reliable (in a statistical, i.e., small standard deviation, sense) estimate of the equilibrium gradient. For the depths and temperature gradients characteristic of the petroleum boreholes in Bolivia and Peru, the AAPG correction leads to equilibrium gradients on average 21% greater than gradients calculated from uncorrected temperatures. A gradient correction of that magnitude is similar to the 15% enhancement noted by *Vacquier* [1984] in the Sergipe-Alagoas Basin of Brazil and the 19% enhancement observed by *da Carvalho et al.* [1980] in the Tertiary Basin of central Sumatra. In both of the latter cases, the equilibrium BHTs were estimated by extrapolation of the cooling trajectory defined by multiple nonequilibrium temperatures obtained at different times after the cessation of drilling. In Figure 3 the uncorrected and corrected temperatures and gradient for the Capahuari group of fields in Peru illustrates the nature of this correction. For other fields shown in Figure 3, only the corrected BHTs and gradients are displayed. As we will show in a later section, the effect of such gradient corrections on the calculation of heat flow in the petroleum fields of Bolivia and Peru is substantially offset by a correction for the effect of pore water on the thermal conductivity of the sedimentary rocks penetrated by the boreholes.

THERMAL CONDUCTIVITY DETERMINATIONS

The laboratory measurements of thermal conductivity were all accomplished using a divided bar apparatus of the type described by *Birch* [1950] but with adaptations as described by *Sass et al.* [1971] to enable the determination of the conductivity of rock chips. We obtained rock samples suitable for disc preparation from almost all of the exploration and mining diamond drill holes in which we made measurements, with the exception of Marcahui in Peru (site 5) and Chilcobija in Bolivia (site 24). At those sites no core was available, but appropriate samples were obtained from nearby outcrops. Over 700 thermal conductivity determinations were made on approximately 600 polished rock discs. All discs were water saturated in vacuum prior to measurement in the divided bar. Repeated measurements of a given disc show variations of about $\pm 2\%$. Discs of some rocks, such as mudstones, may disintegrate upon saturation and were first measured dry before attempting saturation.

Thermal conductivities of the sedimentary rocks encountered in the petroleum fields were determined principally from rock chips collected by the petroleum companies at the time of drilling; a few discs from cored sections supplemented the chip samples. For determining the conductivity of rock chip aggregates, we have used the measurement technique of *Sass et al.* [1971]. As with rock discs, we saturated the chips in vacuum prior to measurement and thus attempted to simulate in situ conditions with respect to porosity and fluids, at least for that part of the porosity with characteristic dimension smaller than the size of the rock fragment, and which may be accessible to saturation via natural permeability. The effect of porosity at larger scales and in situ fracture porosity are undetectable in these measurements, as well as in the disc measurements.

The effects of porosity on the thermal conductivity of the sediments has been thoroughly treated recently by *Vacquier* [1984]. We have been guided by this approach generally but have made some modifications to accommodate the special circumstances of our investigation. The procedure we followed comprises four steps: (1) select a porosity versus depth relationship for each of the principal lithologies encountered in the stratigraphic column; (2) calculate the mean porosity of each lithology over the depth range of the BHTs used to estimate the temperature gradients; (3) using the mean porosity so determined, calculate the conductivity of each porous lithology (assuming water occupies the pore space); and (4) using the conductivities of the individual porous lithologies, estimate the weighted (harmonic) mean conductivity of the stratigraphic column, with the fractions of the column thickness represented by each lithology serving as the weighting factors.

The principal lithologies encountered in the petroleum fields of Bolivia and Peru are overwhelmingly marine and nonmarine clastics, i.e., sandstones and shales in regionally varying proportions. *Vacquier* [1984] presents porosity versus depth relationships for these lithologies, and *Bond and Kominz* [1984] give similar empirical relationships derived from an

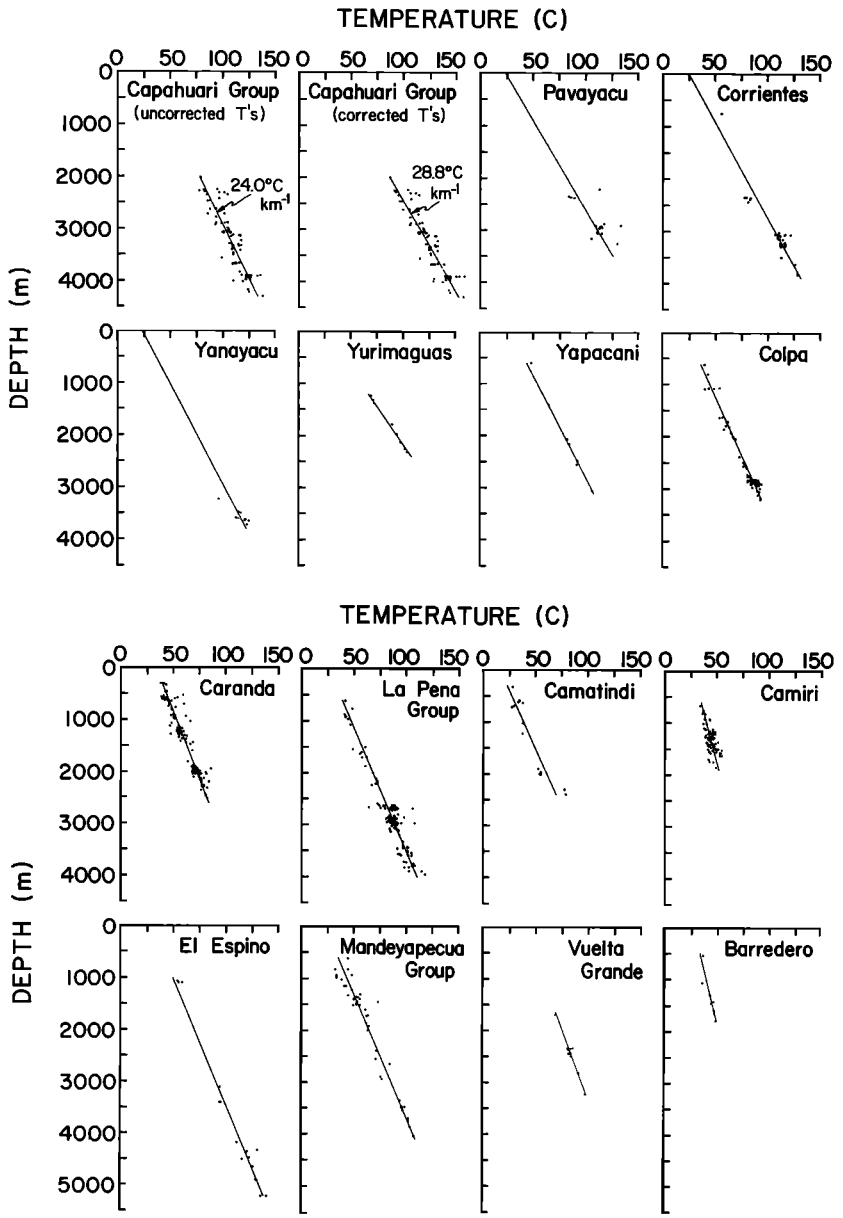

Fig. 3. Bottom hole temperatures and gradients in petroleum fields of Peru and Bolivia. For the Capahuari group of fields both uncorrected and corrected (for drilling disturbance) data are shown; for other fields only corrected data are shown. Least squares line is displayed over depth interval used in heat flow calculation; gradient extending to surface indicates that surface temperature was used in regression.

even larger body of data. Because the Bond and Kominz summary represents a larger and perhaps more diverse data set, we have selected their porosity relationships to apply to our conductivity determinations. The depth range from which most of the BHT observations were obtained is 1–3.5 km, and the mean porosity over this depth interval is likely to be in the range 10–20% for virtually any mixture of clastic lithologies.

Sass et al. [1971] outline the theory and methodology by which measurements of thermal conductivity of rock chips that compose the matrix of a porous rock can be corrected for the effects of the contained pore water and thus yield the conductivity of the saturated porous rock. The correction factor depends on both the actual matrix conductivity and the porosity, but more strongly on the latter. Vacquier determined values of 5.43 and 2.34 W m^{-1} K^{-1} for the matrix conductivities of sandstone and shale, respectively, giving a conductivity ratio of 2.32. We arrive at somewhat lower values of 4.03 and 1.84 W m^{-1} K^{-1} for sandstone and shale, respectively, yielding a conductivity ratio of 2.19 for these lithologies. There is, of course, no reason that our pure matrix values should be the same as those determined by Vacquier; the matrices may have different mineralogies and different fractions of grains and cement. These conductivity values, and 0.607 W m^{-1} K^{-1} for the conductivity of water, yield porous rock conductivity correction factors of 0.79 and 0.81 for sandstone and shale, respectively; i.e., the conductivities for water-saturated sandstones and shales in the depth range of the temperature measurements are 79% and 81% of the pure matrix conductivities, respectively. Clearly, the correction factor in this depth (porosity) range is rather insensitive to the particular lithol-

ogy, and it follows that the correction factor for a stratigraphic column comprising an arbitrary mixture is likewise rather uniform, at about 0.80.

The uncertainties associated with the determination of the harmonic mean conductivity for a sedimentary column derive from several sources: the representativeness of the selected porosity versus depth curves for the respective lithologies, the matrix conductivities of the pure lithologies, the experimental errors in the divided bar measurements, the subdivision of the column into formations or lithologies and the number of samples from each formation or lithology. We have attempted to estimate the uncertainty of each and the internal consistency of our procedures. For the depth range we consider, use of the porosity relationships and matrix conductivities of Vacquier leads to a porosity correction factor of 0.70 and 0.85 for sandstone and shale, respectively, which for the characteristic mix of the two lithologies encountered in the stratigraphy of the Bolivian and Peruvian petroleum fields yields correction factors between 0.77 and 0.82, clearly not significantly different from the nearly uniform value of 0.80 we have determined. Repeated conductivity determinations of the same sample in the divided bar typically yield variations of about $\pm 2\%$ for solid discs and $\pm 5\%$ for fragments. However, because the errors are random, the mean conductivity of a number of samples within a given formation or over a depth range fluctuates much less in a series of repeated measurements than the uncertainty of an individual sample. Finally, we have compared the harmonic mean conductivity of a column, determined from formation thicknesses and characteristic formation conductivities, with the column conductivity, determined from shale and sandstone proportions and characteristic lithologic conductivities, and find the comparison remarkably similar. This consistency of results that we observe is probably not testimony to superior experimental methods and data but rather to the strong averaging effects displayed by the typical stratigraphic sections we have investigated.

A possible source of systematic error relates to the anisotropy of shale thermal conductivity, which has minimum and maximum values perpendicular and parallel to the bedding, respectively. The conductivity of an aggregate of randomly oriented shale fragments determined in the laboratory, therefore, will lie between the maximum and minimum. *Blackwell and Steele* [1981, 1988] have pointed out that in flat-lying undeformed shale beds, the direction of minimum conductivity is vertical, and therefore the laboratory determination will overestimate the in situ effective conductivity and yield an erroneous heat flow. Since the conductivity anisotropy of shales is typically in the range of 15–30%, overestimates of conductivity up to 15% could result. However, in structurally complex settings, such as those encountered in many of the sub-Andean petroleum fields, beds are faulted, folded, and tilted, and the possible effects of shale anisotropy are therefore less pronounced. The mean conductivity of the full rock column in a given borehole or field is of course dependent on the proportions of shale and other lithologies present. The region where anisotropy considerations would potentially have most relevance would be in the petroleum fields of northeastern Peru, where sand/shale ratios average about 1:4, and structural complications are few. In that setting an overestimate of conductivity (and therefore of heat flow) of some 10% is a possibility. In the Bolivian petroleum fields, however, the stratigraphic section is dominated by coarse clastics with a sand/shale ratio of 4:1, and the structural setting is complex. Therefore shale anisotropy probably has no significant effect on the Bolivian heat flow values we report.

HEAT FLOW CALCULATIONS

Methods of Calculation

The values of heat flow established in this investigation have been determined in three ways. At sites with well-established temperature-depth profiles that either are sufficiently far below the local topography to avoid horizontal components of heat flow or are overlain by moderate topography which does not induce significant horizontal components, the heat flow has been calculated by the mean interval heat flow method and/or the Bullard method [*Bullard*, 1939]. In the interval method a heat flow is calculated for each 10-m interval of a borehole as the product of the temperature gradient and mean conductivity of the interval. The mean of the interval heat flows is then the borehole heat flow. In the Bullard method the heat flow is obtained as the slope of the best fitting line to a plot of temperature versus the thermal resistance integral. Heat flows determined by either of these methods are coded 1 in Table 1, and the uncertainties shown are the standard error of the mean heat flow or of the slope of the Bullard plot.

At sites where topography imparts a significant signature at the depths of the temperature measurements, heat flow is determined by a numerical method [*Henry and Pollack*, 1985] that simultaneously treats both topographic and subsurface structural effects on the temperature field and yields the single best fitting value of regional heat flow consistent with a distributed suite of temperature observations. The method, while applicable to the common situation of temperature observations in isolated vertical boreholes, is particularly suited to determining heat flow from an ensemble of observations in inclined boreholes and in horizontal holes or tunnels within mines, in which vertical variations in temperature appear only indirectly through the variable depth of the observation level beneath the surface topography. The numerical modeling procedure comprises solving the three-dimensional heat conduction equation by finite difference techniques, adjusting the regional heat flow until a best fit to the ensemble of temperature observations is achieved. The great majority of sites in the high Andes required a topographic correction, with the site heat flow emerging from the numerical modeling. Sites at which heat flow was determined in this manner are coded 2 in Table 1, and the uncertainties shown are related to the narrowness of the residual minimum obtained in the numerical method.

We also applied this methodology to nine Andean sites reported by Uyeda and colleagues [*Uyeda and Watanabe*, 1982] for which topographic information was available. Revised values for seven sites are shown in Table 1; values at Casapalca and Corocoro were judged "indeterminate," the former because of the suspicion of hydrologically perturbed temperatures as discussed earlier and the latter because of an insufficient number of temperature and conductivity measurements to yield a reliable estimate of heat flow. Two sites, Cerro Verde and Catavi, were visited both by Uyeda and colleagues and by us. At Cerro Verde we were able to make measurements in 17 boreholes, whereas only two were available to Uyeda et al. Our value of heat flow, corrected for

topography, is 18% greater than their earlier uncorrected estimate. At Catavi, each group made measurements in nine horizontal boreholes in different areas. The measurements of Uyeda et al. were principally in the interior of the Salvador stock, an intrusive body with high thermal conductivity. Our measurements were all at the boundary of the stock with the surrounding lower conductivity mudstones, sandstones, and graywackes into which the stock had been intruded. Our calculation of the heat flow made use of both data sets and revealed a lower regional heat flow than that reported from the earlier measurements in the stock alone. The numerical modeling revealed the high conductivity stock as a "chimney," with a high heat flux unrepresentative of the region as a whole.

A third method of calculating heat flow, applicable to sites in the sub-Andean petroleum fields, employs the equation

$$q = \frac{T_2 - T_1}{z_2 - z_1}\left[\sum_{i=1}^{n} f_i/K_i\right]^{-1}$$

where T_1 is the temperature at the top and T_2 is the temperature at the bottom of the stack of n strata, $z_2 - z_1$ is the full thickness of the stack, and f_i is the fraction of the total thickness represented by a given layer. The heat flow q is seen as the product of the average temperature gradient over the entire interval times the bracketed term which is the harmonic mean conductivity of the sedimentary section. *Vacquier* [1984] recommends applying this equation to the calculation of heat flow in individual boreholes and then determining a mean heat flow for the field from the several individual values. Such a procedure is possible only when stratigraphic data are available for every borehole, a condition generally not met in our investigation.

We adopt a generalization of the above for determining the characteristic heat flow of an oil field using data from a number of boreholes in the field. For the "temperature gradient" factor we use the slope of the best fitting line of BHTs from the many boreholes, and for the "conductivity" factor we use the harmonic mean conductivity of the stratigraphic column characteristic of the particular field. Thus we arrive at a characteristic heat flow not for an individual borehole, but for the entire oil field, typically representing an area of about 100 km^2. In some cases we have even grouped several nearby fields with similar stratigraphy into a single analysis. Heat flow values for oil fields determined in this manner are coded 3 in Table 1, and the uncertainties shown in Table 2 derive from the respective uncertainties in gradient and harmonic mean conductivity discussed earlier. The estimated uncertainty of the petroleum field heat flow determinations equals or exceeds the uncertainties of all the conventional determinations shown in Table 2, with the single exception of our revision of the value of *Watanabe et al.* [1980] at site I. The lower level of confidence in heat flows determined using BHTs, well cuttings, and generalized stratigraphy is consistent with a widespread concensus among investigators that such determinations are generally of lesser quality than conventional measurements.

Uplift and Erosion Correction

In areas such as the Andes which are actively undergoing uplift and erosion it is likely that the temperature distribution at shallow depths is not in a steady state because it must be continuously readjusting to the new surface conditions. Analytically, the effect of uplift and erosion may be addressed with the equation of heat conduction in a moving solid, a relevant solution of which is given by *Carslaw and Jaeger* [1959, p. 388]. The variables which must be known in order to calculate the uplift and erosion correction include the present elevation, the time interval over which the uplift and erosion have taken place, the mean erosion rate over that time interval, and the temperature variation on the surface. An atmospheric lapse rate of -5.5 K km^{-1} and a surface temperature at sea level of 25°C have been assumed as valid for past times. A variety of geologic information, including radiometric and fission track ages, fluid inclusions, geomorphology, stratigraphy, and paleontology, provide the necessary constraints on the amount of uplift and/or erosion and on the interval of time in which the processes were active (see *Henry* [1981] for a fuller discussion). Uplift and erosion corrections were applied to all Andean sites except sites 1, 2, and 3 along the north coast of Peru which are at only 200-m elevation and sites 20, 21, 25, and H on the Altiplano where sedimentation has to some extent offset the effects of uplift and erosion. No corrections were applied to any petroleum field sites because of the much greater depths at which temperatures were measured.

DISCUSSION

The best estimates of the heat flow at the sites in Peru and Bolivia are shown in Figure 1*b*, in relation to the major tectonic elements of the region. Some general patterns are immediately apparent: values throughout Peru are less than 60 mW m^{-2} (with the single exception of 66 mW m^{-2} at Toquepala), whereas higher values, in the range 70–125 mW m^{-2}, are confined to the Altiplano and Cordillera Oriental of Bolivia. The heat flow in the sub-Andean petroleum fields of both Boliva and Peru generally cluster between 50 and 60 mW m^{-2}, although two lower values (33 mW m^{-2} at Camiri and 27 mW m^{-2} at Barredero) are observed. A second display of the observations can be seen in Figure 4, which shows heat flow versus distance from the Peru-Chile trench. This display includes the terrain-corrected value for the site in Ecuador [*Uyeda et al.*, 1980] and the mean values from Lake Titicaca [*Sclater et al.*, 1970]. Low values, in the range of 20–45 mW m^{-2}, are observed within 200 km of the trench, similar to the low heat flow generally observed in this tectonic setting elsewhere. The higher heat flow of Bolivia is situated immediately to the east of the arc of Quaternary volcanoes, thus revealing a "back arc" heat flow high similar to that observed in many of the western Pacific marginal basins as well as in the regions to the east of the Cascade and Mexican volcanic arcs in North America [*Watanabe et al.*, 1977; *Blackwell et al.*, 1982; *Ziagos et al.*, 1985; *Lewis et al.*, 1985]. There appears to be no evidence, however, for the existence of high heat flow in Peru in the equivalent distance range from the trench, although admittedly the data are few. However, Quaternary volcanism is also absent from Peru except in the extreme south, thus reinforcing the suggestion that the tectonic setting characterized by both Quaternary volcanism and a back arc heat flow high is not representative of most of present-day Peru.

A likely explanation for this contrast can be found in the configuration of the subducted Nazca Plate beneath Peru and Bolivia. Abundant seismicity has enabled the mapping of the upper surface of the Nazca Plate [*Stauder*, 1973, 1975; *Barazangi and Isacks*, 1976, 1979; *Hasegawa and Sacks*, 1981], revealing a 25°–30° dip of the subduction zone beneath Bolivia, and a much shallower subhorizontal subduction beneath central and northern Peru. The transition between the two zones

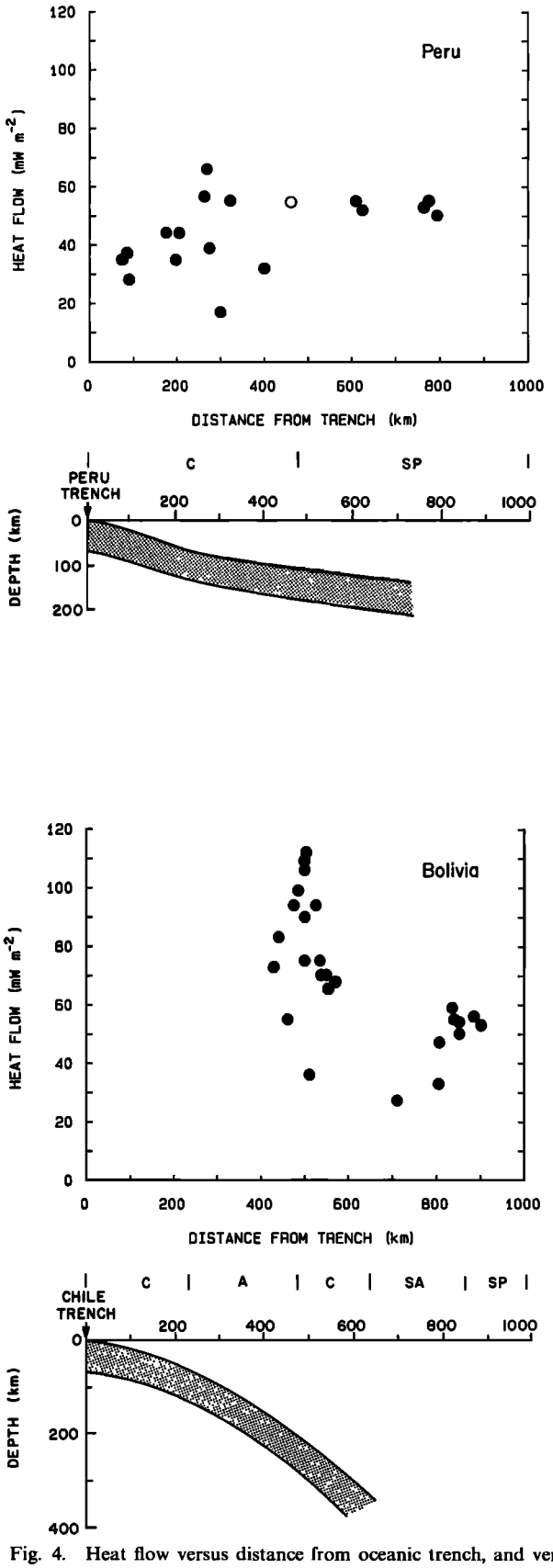

Fig. 4. Heat flow versus distance from oceanic trench, and vertical cross sections showing configuration of subducted oceanic lithosphere [after *Barazangi and Isacks*, 1976], for (top) Peru and (bottom) Bolivia. Transition from shallow to steeper dip occurs in southernmost Peru. Open circle in Peru data represents mean value from Lake Titicaca (*Sclater et al.* [1970]; site T of Figure 1). Tectonic codes shown are defined in Figure 1.

occurs in southern Peru and has been variously described as a tear or contortion in the Nazca Plate (see *Schneider and Sacks* [1987] for a recent discussion). Apparently, the mantle wedge between the continental and oceanic lithosphere in Bolivia has experienced some convection induced by the descending Nazca Plate, thereby augmenting the surface heat flow. Beneath Peru the subhorizontal subduction has effectively created a cold underplate to the overlying lithosphere, which extracts heat from its surroundings and interrupts the flow of heat from greater depths, thus producing a zone of low heat flow across all of Peru.

The widespread existence of Miocene volcanics in central and northern Peru [*Noble et al.*, 1974] suggests that the Miocene subduction there was more like that beneath present-day Bolivia, i.e., more steeply dipping, volcanogenic, and with an active mantle wedge causing high surface heat flow. If that interpretation is correct, then the present-day subhorizontal subduction in the region is a post-Miocene development. Such a scenario has implications for the time scale of the transition from presumed high heat flow in the Miocene associated with an active mantle wedge to the low heat flow across Peru in the present day. The lithosphere above the subhorizontal Nazca Plate is in the 75- to 125-km range of thickness. The thermal conductive time constant for a slab of this thickness [*Lachenbruch and Sass*, 1977] is much greater than the 10–15 Ma since the cessation of Miocene volcanism and the presumed change in subduction angle which initiated the present-day subhorizontal cold underplate.

A possible solution to this problem would be the production of the Miocene volcanics by partial melting of the subducting plate, but with a stable mantle wedge which resisted convection induced by the subducting plate. This solution circumvents the problem of a rapid reduction in heat flow by rendering inoperative the mechanism by which back arc heat flow highs are thought to be produced, in effect arguing that the tectonic setting in central and northern Peru in the Miocene was significantly different from that beneath Boliva in the present day. An alternative solution would be the existence of a thinner lithosphere with a suitably shorter time constant so that the transition to lower heat flow could have taken place in the post-Miocene interval. This solution at first appears to solve one problem only by introducing another, i.e., finding a mechanism to thicken the lithosphere beneath Peru in the same time interval as the heat flow diminishes. However, just such a process has recently been suggested for the subduction of the Juan de Fuca Plate beneath Vancouver Island and western British Columbia [*Spence et al.*, 1985; *Greene et al.*, 1986; *Clowes et al.*, 1987]. There deep seismic reflections have revealed an imbrication of two subducted oceanic slabs, one under the other, thus doubling the lithospheric thickness. Such a process would place a cold underplate high in the section early, followed by a second underplate at a later time.

Equivalent seismic investigations that could determine if such a process might have occurred beneath Peru have not been carried out. However, a suggestion that the Nazca Plate may be about to initiate a new subduction zone at the Peruvian trench [*Hussong et al.*, 1976] lends indirect support to this hypothesis. Detailed thermal models of the underplating process including the effects of imbrication are under way and will be reported in a subsequent paper.

Acknowledgments. Principal funding for this project was provided by the U.S. National Science Foundation (grants EAR 78-09131 and

INT-8016941). Additional funding was provided by the University of Michigan Department of Geological Sciences (Scott Turner Fund), the Carnegie Institute of Washington Department of Terrestrial Magnetism (H. O. Wood Fund), and the Geological Society of America (research grant 2462-79). Excellent logistical support in Bolivia was provided by the Servicio Geologico de Bolivia (GEOBOL). We acknowledge with gratitude the active cooperation of Daniel Huaco and Leonidas Ocola of the Instituto Geofisico del Peru, Father Ramon Cabre of the Observatorio San Calixto, Ings. Wilfredo Vargas, Miguel Acef, Freddy Rodriguez, Jaime Telleria, and Pascual Arequipa of GEOBOL, Ing. Guillermo Villa of the Universidad Nacional de San Agustin, and Ings. Jose Telleria and Eloy Martinez of the Universidad Mayor de San Andres. We thank the following organizations and companies for their cooperation in various aspects of the investigations: PETROPERU, CENTROMIN, MINEROPERU, INGEMET, The Spanish Mission, and Southern Peru Copper Corporation, all in Peru, and Yacimientos Petroliferos Fiscales Bolivianos (YPFB), Corporacion Minera de Bolivia (COMIBOL), Comision Boliviana de Energia Nuclear (COBOEN), Instituto de Investigaciones Fisicas, all in Bolivia, and Gulf International Petroleum Company. Wei Dawei assisted with the thermal conductivity measurements. Last but not least we thank Krystyna Swirydczuk and Icaro Vitorello for their many contributions and moral support both in the field and in other aspects of the project.

REFERENCES

American Association of Petroleum Geologists, Basic data file from AAPG geothermal survey of North America, Univ. of Okla., Norman, Okla., 1976.

Barazangi, M., and B. Isacks, Spatial distribution of earthquakes and subduction of the Nazca plate beneath South America, *Geology*, *4*, 686–692, 1976.

Barazangi, M., and B. Isacks, Subduction of the Nazca plate beneath Peru: Evidence from spatial distribution of earthquakes, *Geophys. J. R. Astron. Soc.*, *57*, 537–555, 1979.

Birch, F., Flow of heat in the Front Range, *Geol. Soc. Am. Bull.*, *61*, 567–630, 1950.

Blackwell, D., and J. Steele, Heat flow determinations in Kansas and their implications for mid-continent heat flow patterns (abstract), *Eos Trans. AGU*, *62*, 392, 1981.

Blackwell, D., and J. Steele, Thermal conductivity of sedimentary rocks—Measurement and significance, in *Thermal History of Sedimentary Basins*, edited by N. Naeser and T. McCulloh, Springer, New York, in press, 1988.

Blackwell, D., R. Bowen, D. Hull, J. Riccio, and J. Steele, Heat flow, arc volcanism, and subduction in northern Oregon, *J. Geophys. Res.*, *87*, 8735–8754, 1982.

Bond, G. C., and M. A. Kominz, Construction of tectonic subsidence curves for the early Paleozoic miogeocline, southern Canadian Rocky Mountains: Implications for subsidence mechanisms, age of breakup, and crustal thinning, *Geol. Soc. Am. Bull.*, *95*, 155–173, 1984.

Bullard, E., Heat flow in South Africa, *Proc. R. Soc. London, Ser. A*, *173*, 474–502, 1939.

Carslaw, H. S., and J. C. Jaeger, *Conduction of Heat in Solids*, 2nd ed., 510 pp., Oxford University Press, New York, 1959.

Clowes, R., M. Brandon, A. Green, C. Yorath, A. Sutherland Brown, E. Kanasewich, and C. Spencer, LITHOPROBE—Southern Vancouver Island: Cenozoic subduction complex imaged by deep seismic reflections, *Can. J. Earth Sci.*, *24*, 31–51, 1987.

da Carvalho, S. H., I. Purwoko, I. Siswoyo, M. Thamrin, and V. Vacquier, Terrestrial heat flow in the Tertiary Basin of central Sumatra, *Tectonophysics*, *69*, 163–188, 1980.

Greene, A., R. Clowes, C. Yorath, C. Spencer, E. Kanasewich, M. Brandon, and A. Sutherland Brown, Seismic reflection imaging of the subducting Juan de Fuca plate, *Nature*, *319*, 210–213, 1986.

Hasegawa, A., and I. S. Sacks, Subduction of the Nazca plate beneath Peru as determined from seismic observations, *J. Geophys. Res.*, *86*, 4971–4980, 1981.

Henry, S. G., Terrestrial heat flow overlying the Andean subduction zone, Ph.D. dissertation, 194 pp., Univ. of Mich., Ann Arbor, Mich., 1981.

Henry, S. G., and H. N. Pollack, Heat flow in the presence of topography: Numerical analysis of data ensembles, *Geophysics*, *50*, 1335–1341, 1985.

Hussong, D., P. Edwards, S. Johnson, J. Campbell, and G. Sutton, Crustal structure of the Peru-Chile trench: 8–12 degrees south latitude, in *The Geophysics of the Pacific Ocean Basin and Its Margin*, *Geophys. Monogr. Ser.*, vol. 19, edited by G. H. Sutton, M. H. Manghnani, and R. Moberly, pp. 71–85, AGU, Washington, D. C., 1976.

Lachenbruch, A., and J. Sass, Heat flow in the United States and the thermal regime of the crust, in *The Earth's Crust*, *Geophys. Monogr. Ser.*, vol. 20, edited by J. Heacock, pp. 626–675, AGU, Washington, D. C., 1977.

Lewis, T., A. Jessop, and A. Judge, Heat flux measurements in southwestern British Columbia: The thermal consequences of plate tectonics, *Can. J. Earth Sci.*, *22*, 1262–1273, 1985.

Noble, D., E. McKee, E. Farrar, and U. Peterson, Episodic Cenozoic volcanism and tectonism in the Andes of Peru, *Earth Planet. Sci. Lett.*, *21*, 213–220, 1974.

Sass, J. H., A. H. Lachenbruch, and R. J. Munroe, Thermal conductivity of rocks from measurements of fragments and its application to heat flow determinations, *J. Geophys. Res.*, *76*, 3391–3401, 1971.

Sass, J. H., R. J. Munroe, and T. H. Moses, Jr., Heat flow from eastern Panama and northwestern Colombia, *Earth Planet. Sci. Lett.*, *21*, 134–142, 1974.

Schneider, J., and I. S. Sacks, Stress in the contorted Nazca plate beneath southern Peru from local earthquakes, *J. Geophys. Res.*, *92*, 13,887–13,902, 1987.

Sclater, J. G., V. Vacquier, and J. H. Rohrhirsch, Terrestrial heat flow measurements on Lake Titicaca, Peru, *Earth Planet. Sci. Lett.*, *8*, 45–54, 1970.

Shen, P. Y., and A. E. Beck, Stabilization of bottom hole temperatures with finite circulation time and fluid flow, *Geophys. J. R. Astron. Soc.*, *86*, 63–90, 1986.

Speece, M. A., T. D. Bowen, J. L. Folcik, and H. N. Pollack, Analysis of temperatures in sedimentary basins: The Michigan Basin, *Geophysics*, *50*, 1313–1334, 1985.

Spence, G., R. Clowes, and R. Ellis, Seismic structure across the active subduction zone of western Canada, *J. Geophys. Res.*, *90*, 6754–6772, 1985.

Stauder, W., Mechanism and spatial distribution of Chilean earthquakes with relation to subduction of the oceanic plate, *J. Geophys. Res.*, *78*, 5033–5061, 1973.

Stauder, W., Subduction of the Nazca plate under Peru as evidenced by focal mechanisms and by seismicity, *J. Geophys. Res.*, *80*, 1053–1064, 1975.

Uyeda, S., and T. Watanabe, Terrestrial heat flow in western South America, *Tectonophysics*, *83*, 63–70, 1982.

Uyeda, S., T. Watanabe, E. Kausel, M. Kubo, and Y. Yashiro, Report of heat flow measurements in Chile, *Bull. Earthquake Res. Inst. Univ. Tokyo*, *53*, 131–163, 1978*a*.

Uyeda, S., T. Watanabe, and F. Volponi, Report of heat flow measurements in San Juan and Mendoza, Argentine, *Bull. Earthquake Res. Inst. Univ. Tokyo*, *53*, 165–172, 1978*b*.

Uyeda, S., T. Watanabe, Y. Ozasayama, and K. Ibaragi, Report of heat flow measurements in Peru and Ecuador, *Bull. Earthquake Res. Inst. Univ. Tokyo*, *55*, 55–74, 1980.

Vacquier, V., Oil Fields—A source of heat flow data, *Tectonophysics*, *103*, 81–98, 1984.

Watanabe, T., M. Langseth, and R. Anderson, Heat flow in back-arc basins of the western Pacific, in *Island Arcs, Deep Sea Trenches, and Back-Arc Basins*, *Maurice Ewing Ser.*, vol. 1, edited by M. Talwani and W. C. Pitman III, pp. 137–162, AGU, Washington, D. C., 1977.

Watanabe, T., S. Uyeda, J. A. Guzman Roa, R. Cabre, and H. Kuronuma, Report of heat flow measurements in Bolivia, *Bull. Earthquake Res. Inst. Univ. Tokyo*, *55*, 43–54, 1980.

Ziagos, J., D. Blackwell, and F. Mooser, Heat flow in southern Mexico and the thermal effects of subduction, *J. Geophys. Res.*, *90*, 5410–5420, 1985.

S. G. Henry, Conoco Incorporated, P.O. Box 2197, Houston, TX 77252.

H. N. Pollack, Department of Geological Sciences, University of Michigan, Ann Arbor, MI 48109.

(Received March 22, 1988;
revised July 28, 1988;
accepted August 17, 1988.)